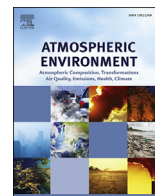




Contents lists available at ScienceDirect

Atmospheric Environment

journal homepage: www.elsevier.com/locate/atmosenv

Diagnosing Tibetan pollutant sources via volatile organic compound observations



Hongyan Li^a, Qiusheng He^{a,*}, Qi Song^a, Laiguo Chen^{b,**}, Yongjia Song^c, Yuhang Wang^c, Kui Lin^b, Zhencheng Xu^b, Min Shao^d

^a School of Environment and Safety, Taiyuan University of Science and Technology, Taiyuan, China

^b Urban Environment and Ecology Research Center, South China Institute of Environmental Science (SCIES), Ministry of Environmental Protection (MEP), Guangzhou, China

^c School of Earth and Atmospheric Science, Georgia Institute of Technology, Atlanta, GA, USA

^d College of Environmental Sciences and Engineering, Peking University, Beijing, China

HIGHLIGHTS

- Industry, biomass burning, and traffic factors for VOCs are identified in Tibet.
- Different source factors present different spacial distributions in Tibet.
- Different source factors have their own specific source regions.
- The results provide support for international protection of Tibetan air quality.

ARTICLE INFO

Article history:

Received 7 March 2017

Received in revised form

9 July 2017

Accepted 17 July 2017

Available online 18 July 2017

Keywords:

Tibet

Volatile organic compounds

Tracers

Sources

Regional transport

ABSTRACT

Atmospheric transport of black carbon (BC) from surrounding areas has been shown to impact the Tibetan environment, and clarifying the geographical source and receptor regions is crucial for providing guidance for mitigation actions. In this study, 10 trace volatile organic compounds (VOCs) sampled across Tibet are chosen as proxies to diagnose source regions and related transport of pollutants to Tibet. The levels of these VOCs in Tibet are higher than those in the Arctic and Antarctic regions but much lower than those observed at many remote and background sites in Asia. The highest VOC level is observed in the eastern region, followed by the southern region and the northern region. A positive matrix factorization (PMF) model found that three factors—industry, biomass burning, and traffic—present different spatial distributions, which indicates that different zones of Tibet are influenced by different VOC sources. The average age of the air masses in the northern and eastern regions is estimated to be 3.5 and 2.8 days using the ratio of toluene to benzene, respectively, which indicates the foreign transport of VOC species to those regions. Back-trajectory analyses show that the Afghanistan-Pakistan-Tajikistan region, Indo-Gangetic Plain (IGP), and Meghalaya-Myanmar region could transport industrial VOCs to different zones of Tibet from west to east. The agricultural bases in northern India could transport biomass burning-related VOCs to the middle-northern and eastern zones of Tibet. High traffic along the unique national roads in Tibet is associated with emissions from local sources and neighboring areas. Our study proposes international joint-control efforts and targeted actions to mitigate the climatic changes and effects associated with VOCs in Tibet, which is a climate sensitive region and an important source of global water.

© 2017 Elsevier Ltd. All rights reserved.

1. Introduction

Tibet, located in the far western area of China and surrounded by the Central Himalayas to the west and south, is one of the most remote areas and the highest plateau in the world (Xiao et al.,

* Corresponding author.

** Corresponding author.

E-mail addresses: heqs@tyust.edu.cn (Q. He), chenlaiguo@scies.org (L. Chen).

2015). Although few direct pollutant emissions have been observed, the environmental conditions of this unique geological and geographical unit have changed in recent decades; these changes manifest as warming trends, glacier retreat and permafrost degradation (Qiu, 2008; Yao et al., 2012; Yang et al., 2014). These changes will influence conditions on the plateau and will affect the water availability for billions of inhabitants in downstream regions distributed across more than 10 countries; they could also impact atmospheric circulation at regional and global scales (Qiu, 2008).

Mounting evidence indicates that the transport of air pollutants that have great importance to the climate system, such as BC and organic acids from surrounding areas, is the primary cause of the changes in the environmental conditions in Tibet except for the increase of greenhouse gases (GHGs) and the associated global warming (Qiu, 2008; Ming et al., 2008; Kaspari et al., 2011; Cong et al., 2015). Surrounded by the largest BC sources of East Asia and South Asia (Bond et al., 2007; Ohara et al., 2007), especially the highly populated and polluted river basin of the IGP (Fig. 1a), Tibet is primarily affected by pollutant transport from these regions (Kopacz et al., 2011; Lu et al., 2012; Zhao et al., 2013; Wang et al., 2015, 2016; Zhang et al., 2015; Li et al., 2016; Kang et al., 2016; Zhang et al., 2017). Identifying the detailed regions from which the BC originates would be valuable in prioritizing mitigation efforts in this pivotal region.

Mainly driven by the wind system, the transport pathways are usually alike for the air pollutants from a common source. Studies about different air pollutants have reported atmospheric transport from the India–Nepal–Pakistan region to Mt. Everest (Li et al., 2006), from western China, Kyrgyzstan, Tajikistan, and Pakistan to western Tibet (Kopacz et al., 2011), from Bangladesh as well as easternnorth-central and northern regions of Indian to south-eastern Tibet (Cao et al., 2010; Wang et al., 2015), from the IGP of southern Asia to central Tibet (Ming et al., 2010; Xia et al., 2011), and even from the former USSR, Middle East, and eastern Europe to Mt. Everest and Tibet (Kaspari et al., 2011; Lu et al., 2012). Although they provide valuable information for the transport of BC, a large part of those studies were just confined to single-site observations. Tibet has an area of 1.2 million km² with complex terrain and variable meteorological conditions. Single-site observation can not

reflect the situation across the whole Tibet. The other part were model simulations, which may have large uncertainties because of poor model resolution in the topographically complex region, lack of in situ and radiosonde observations, potential inaccuracies in emission inventories, and uncertainties in precipitation frequency (Zhang et al., 2017; Kopacz et al., 2011). Therefore, a good spatial-coverage in situ investigation needs to be done to construct a clearer source-receptor relationship of air pollutants in Tibet before developing out effective protection measures.

VOCs are a group of atmospheric pollutants which have similar sources to BC such as biomass burning, traffic exhaust, and industrial processes (Sarkar et al., 2014; Kopacz et al., 2011). Many individual VOCs have common sources, sometimes have unique, source specific relationships to one another. Their lifetimes, ranging from a few hours to several weeks, are comparable to regional and intercontinental transport times of air masses. These features make the combination of specific tracers and the ratios between them have strong utility to identify emission source types, regions, and related atmospheric transport (Baker et al., 2011; Helmig et al., 2008; Shim et al., 2007; Wang et al., 2003). Therefore, we apply in this study the measurements of VOCs sampled across the whole Tibet to diagnose the sources regions and related transport of pollutants to Tibet.

Considering the source type or composition at each sampling site may be different due to the uneven distribution of human activities and the associated emission sources of pollutants no matter in local or upwind regions, factor analysis using the PMF method is applied to our measurements of the VOCs tracers (Sect. 2.4). PMF is an advanced multivariate factor analysis tool that can decompose a matrix of speciated sample data into two matrices: factor contributions (G) and factor profiles (F) (US EPA, 2014). Because the factor analysis is based on the interdependencies between observed variables, the tracers indicating a similar source type or source locations will be grouped together to one factor. Thus, this method can explain the variability of tracer species concentrations by a few underlying source factors. No prior assumptions, such as meteorological conditions prevailing at the measurement sites, is required for this application. PMF can also provide the normalized contribution per sample of each factor, so we use it to explore the

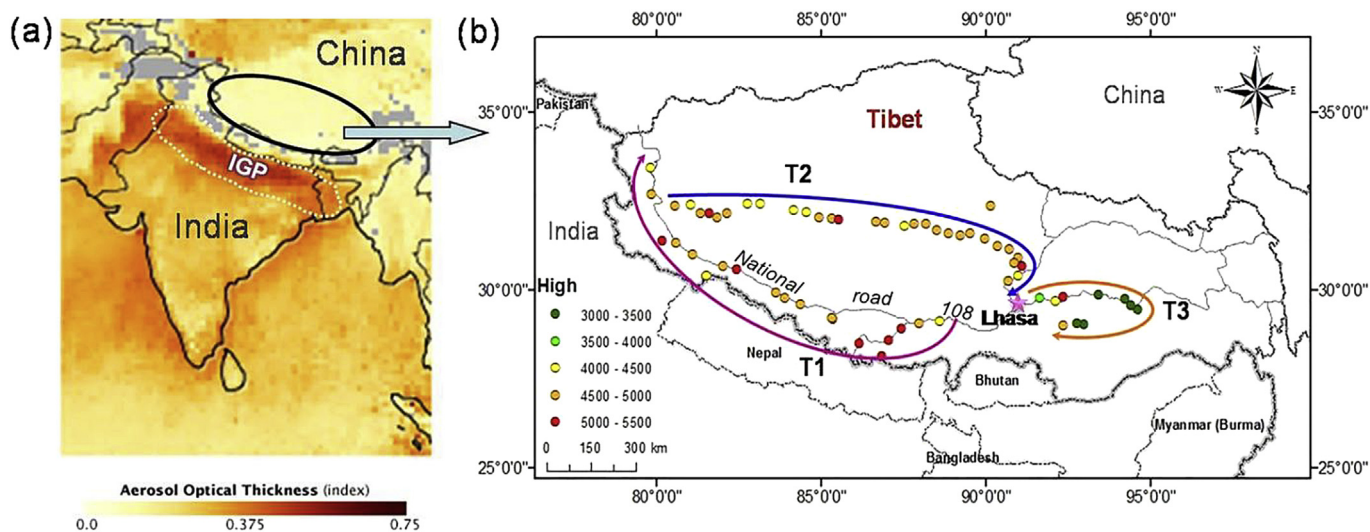


Fig. 1. (a) Location of the area of measurement in Tibet. The colors indicate the Aerosol Optical Thickness derived from data obtained from the Multi-angle Imaging Spectroradiometer (MISR) instrument on NASA's Terra spacecraft from 1 Mar 2000 to 30 Nov 2008; (b) Geographical map of Tibet that shows the sampling tracks in this study, which are ordered from T1 (Track 1, purple arrow line) to T2 (Track 2, blue arrow line) and then to T3 (Track 3, orange arrow line). The different colored dots represent the different altitudes (dark green, 3000–3500 m; light green, 3500–4000 m; light yellow, 4000–4500 m; orange, 4500–5000 m; and red, 5000–6000 m). (For interpretation of the references to colour in this figure legend, the reader is referred to the web version of this article.)

distribution of the source factors in Tibet in this study. Then, the photochemical processing and air mass ages are discussed, and the source regions for each factor are traced using the Hybrid Single Particle Lagrangian Integrated Trajectory (HYSPPLIT) model.

2. Sampling and analysis

2.1. Sampling locations

Fig. 1b shows the locations and tracks in Tibet where samples were collected, and the sampling sites at different altitudes are indicated by different colors. According to the sampling order, all of the sampling sites are divided into three groups (T1–T3), and they are numbered as shown in Table S1, with Lhasa (the capital of Tibet) as the reference crossing. Using Lhasa as a reference, the label T1 refers to the southwestern area, which presents an average altitude of approximately 4500 m and includes the national road 108; the label T2 refers to the northwestern area, which presents an altitude of approximately 4000 m, does not include roads, and has a low population; and T3 refers to the eastern area, which has a lower altitude than T1 and T2 (3000–4000 m) and presents a greater amount of human activities. The number of samples for areas T1, T2, and T3 are 19, 29, and 12, respectively. All of the sampling sites were located in remote areas with few anthropogenic activities. The sampling was conducted from 13 to 25 October 2010, with the samples being taken in daytime from 08:00 to 19:00 LT (Beijing time, GMT C 8) with an interval of 1–2 h. The detailed time of sampling and geo-location information for each sampling site are presented in Table S1. Most of the sampling sites were located on the tops of mountains, and presented open horizons and breeze wind speed. The presence of vehicles was avoided. The meteorological parameters were recorded for each sampling site.

2.2. Sample collection and chemical analysis

In this study, 2-L electro-polished stainless-steel canisters were used to collect all of the air samples. During sampling, dust and particulate intrusion was prevented by fixing a restricted grab sampler (39-RS-x; Entech Instruments; 2207 Agate CT, Simi Valley, CA) to the inlet of the canister. This sampler has a 5- μm Silonite-coated metal particulate filter. The sampling rate was controlled by the valve, and the collection time was more than 5 min. The filled canisters were transported back to the laboratory at the Guangzhou Institute of Geochemistry, Chinese Academy of Science, and analyzed within 1 month after collection. The samples were pretreated by a preconcentrator (Entech Instruments Inc., USA) and analyzed using a gas chromatography-mass selective detector (Agilent 7890A/5973N, USA) using two different column/detector combinations to concurrently analyze both low- and high-boiling-point VOCs with each injection. The detailed analytical procedure was introduced by Zhang et al. (2012).

2.3. Quality control and quality assurance (QA/QC)

Before transport to the sampling sites, all canisters were cleaned and vacuumed according to the TO-15 method of the U.S. Environmental Protection Agency (EPA). After the cleaning procedures, all vacuumed canisters were re-filled with pure nitrogen, stored in the laboratory for at least 24 h, and then analyzed the same methods as field samples to check if there was any contamination in the canisters. Only if all the target VOC compounds were not present, the canister was used to collect the air sample.

Target compounds were identified based on their retention times and mass spectra, and quantified by external calibration methods. C_4 – C_{10} hydrocarbons were determined based on MSD

signals, while C_2 and C_3 hydrocarbons were determined based on FID signals. The calibration standards were prepared by dynamically diluting the Photochemical Assessment Monitoring Stations (PAMS) standard mixture and TO-15 standard mixture (100 ppbv, Spectra Gases Inc., New Jersey, USA) to 0.5, 1, 5, 15 and 30 ppbv. The calibration curves were obtained by running the five diluted standards, plus humidified zero air, the same way as the field samples. The concentration-response (peak area) correlation coefficients were 0.992–0.999. The analytical system was checked daily with humidified zero air to ensure that it was clean, and then a one-point (typically 1 ppbv) calibration before running air samples. If the response was beyond $\pm 10\%$ of the initial calibration curve, recalibration was performed. The measurement precision was determined by repeated analysis of a standard mixture (1 ppbv) seven times, and controlled within 5%, respectively.

2.4. PMF analysis

PMF 5.0 software (provided by the U.S. EPA) is used for the source apportionment in this study, and the detailed principles and applications are described in the user guide (US EPA, 2014) as well as in previous studies (Sarkar et al., 2017; Liu et al., 2016; Mo et al., 2017). A suite of VOC species is selected to resolve the VOC sources with low uncertainty according to the following principles: (1) species that are not indicative of any source are not included; (2) species with more than 50% of their concentration values missing or that fell below the MDLs are excluded; (3) species with very short atmospheric lifetimes are rejected; and (4) species that are poorly fitted by the PMF model are discarded. Finally, 10 species including ethyne, propene, propane, i-pentane, 2-methylpentane, benzene, toluene, ethyl-benzene, xylene (BTEX), and methyl chloride (CH_3Cl) are chosen. These species all have good tracer properties and represent species of common concern in the atmosphere. Ethyne is considered an excellent tracer for long-range pollution transport and incomplete combustion (Blake et al., 2003). Propene and propane are tracers of smoldering combustion from forest clearing and shifting agricultural practices (Ferek et al., 1998; Greenberg et al., 1984). Isopentane is a typical tracer for traffic-related emissions (Shim et al., 2007; Rubin et al., 2006), and 2-methylpentane is a tracer for gasoline evaporation (He et al., 2015). BTEX represent good tracers for industrial sources, and benzene is also a good tracer for biomass burning and vehicle exhausts (Tang et al., 2008). CH_3Cl is an important indicator for biomass burning emissions (Shim et al., 2007).

In the PMF application, all of the data from T1, T2 and T3 zones are included as a unique input database. Each missing value is replaced by the median value of the species, and its uncertainty is set to four times the median value. Data with values below the method detection limit (MDL) remain unchanged, and the uncertainty is calculated as follows (Eq. (1)):

$$\text{Unc} = \frac{5}{6} \times \text{MDL} \quad (1)$$

The uncertainty for the data greater than MDL is calculated by using the measurement uncertainty (MU, 10%, the maximum possible uncertainty in our study) and the MDL based on Eq. (2):

$$\text{Unc} = \sqrt{(\text{MU} \times \text{concentration})^2 + 0.5 \times (\text{MDL})^2} \quad (2)$$

To determine the optimal number of sources, three to six factors are examined. Twenty base runs are conducted, and the best-modeled number of factors is determined by the Q values, the scaled residuals distributions, and the interpretability of the resulting source profiles. For our data, three factor solution is found

to be the most appropriate. In the selected base run solution, ratios between Q (true) and Q (robust) are within 1.05. Most of the scaled residuals are nearly normally distributed within the range of +3 and -3, which represents a good model fit. The uncertainty associated with the PMF solution is estimated by the methods of classical bootstrap (BS), displacement of factor elements (DISP), and bootstrap enhanced by displacement (BS-DISP). The results show that all factors are mapped in >90% of BS runs, there are no swaps with DISP, and 100% of the BS-DISP runs are successful, which indicate the solution is stable at three factors. Then, the PMF results are adjusted by setting various Fpeak values from -5 to +5 to reduce the rotational ambiguity and explore more realistic profiles. In our study, an F peak value of -1 for the 3-factorial solution offers the most physically reasonable solution.

2.5. Back-trajectory calculations

The HYSPLIT model is the most widely used atmospheric transport and dispersion model in the field of atmospheric sciences (http://www.arl.noaa.gov/HYSPLIT_info.php), and it is used here to track the emission trajectories. This model has the ability to calculate simple air mass trajectories and simulate transport, dispersal, chemical transformation, and deposition. The trajectory calculation in HYSPLIT is conducted by spatio-temporally integrating the particle position vectors based on the particles passively following the wind. The next position is calculated from the average speed at the previous position and the first-guess position. The frequency of the back trajectory point is 1 h; the total period is 120 h (5 days). The trajectory error varies from 15 to 30% of the travel distance because of inaccurate input data, integration computational errors, and the resolution errors (http://www.arl.noaa.gov/documents/workshop/NAQC2007/HTML_Docs/trajerro.html). Resolution errors are usually much larger than integration errors. The accuracy and quality of the input meteorological data are critical for calculating the trajectory. NOAA's Climate Forecast System Reanalysis (CFSR) data (the finest resolution data) are the best option for our research domain (the Tibet Plateau). An effective method of reducing the resolution error is to run trajectories from the same location using several different vertical levels, and this method has been applied in this study. The computation integration error of a backward trajectory in HYSPLIT document indicates about 1 km horizontally and 13 m vertically after a 136-hour integration time.

3. Result and discussion

3.1. Ambient levels of VOCs in Tibet

The hydrocarbon species levels (minimum, maximum, and mean) observed in our study are listed in Table 1, and they are compared with those in previous studies. The levels for all of the species in Tibet are higher than those of the Arctic and Antarctic regions (Hellén et al., 2012), although they are much lower than those observed at many remote and background Asian sites, such as Mt. Tengchong and Mt. Jianfeng in China, the Oki Islands of Japan, Mt. Nagakot in Nepal, Hok Chuen in Taiwan, Mt. Abu in India (Tang et al., 2009 and references therein), and Sukmo Island in Korea (Choi et al., 2010). The values are comparable with the data from TaiO site in Hong Kong (Wang et al., 2005), which represents an underpopulated coastal region with few local emissions, but the atmosphere has been influenced by anthropogenic activities because of the proximity of several large urban centers. Tibet presents similar conditions.

Among the different areas of Tibet, the VOC species all have the

Table 1 Comparison of the average mixing ratios of hydrocarbons at various rural or remote sites worldwide (pptv).

Hydrocarbons	Tibet (this study)		Jianfeng Mou, China ^a		Tengchong Mou, China ^a		Sukmo Island Korea ^b		Oki Islands, Japan ^a		Nagakot Nepal ^a		Heng-Chuen Taiwan ^a		TaiO Hong Kong ^c		Mt.Abu India ^a		Arctic ^d		Antarctic ^d	
	Oct2010		Apr–May 2004		Apr–May 2004		Apr–May 2004		Jul–Aug 1998		Nov 1998		Oct 2002		Aug2001–Dec2002		Apr 2002		Aug–Sep 2008		Dec–Jan 2007–2008	
	Min	Max	Min	Max	Min	Max	Min	Max	Min	Max	Min	Max	Min	Max	Min	Max	Min	Max	Min	Max	Min	Max
Ethyne	57	479	390	144	780	144	855	200	200	520	400	400	142	880	56	16						
propene	24	160	110	45	170	45	130	110	110	140	700	56	160	160	56	10						
Propane	22	227	170	72	230	72	1000	160	160	250	900	93	440	440	56							
i-Pentane	0	282	200	76	150	76	332	60	60	60	1300	56										
2-methylpentane	1	128	34	34		34	108	18	18		400	25										
Benzene	3	107	130	21	240	21	237				300	49										
Toluene	1	87	170	26	160	26	641				900	70										
Ethylbenzene	0	29	20	8	30	8	73				200	20										
m/p-Xylene	0	45	40	10	60	10	99				300	66										
o-Xylene	0	27	BDL	6	30	6	58				300	30										

^a Tang et al. (2009) and references therein.
^b Choi et al. (2010).
^c Wang et al. (2005).
^d Hellén et al. (2012).

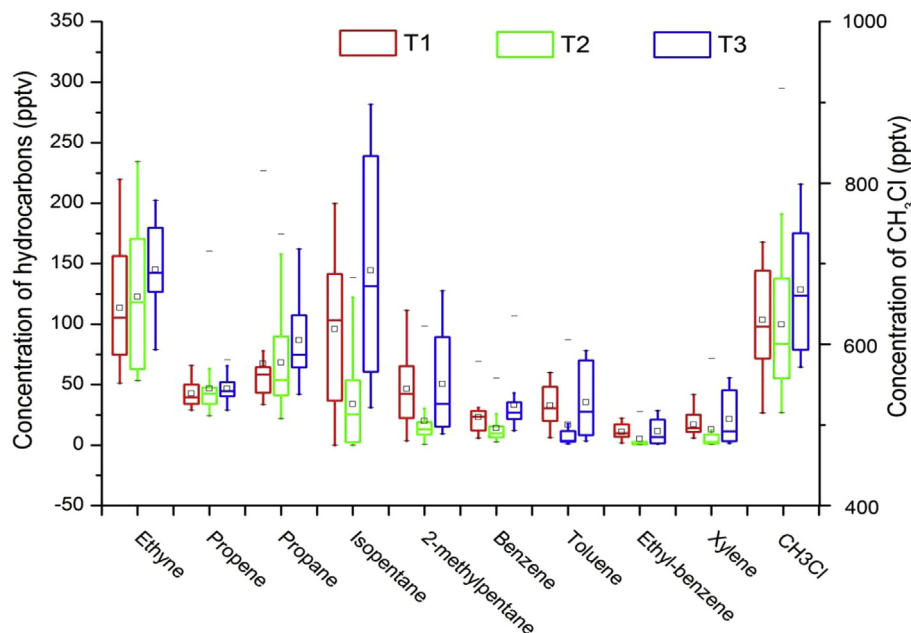


Fig. 2. Box plots of the VOC concentrations in the different zones of Tibet. The upper and lower error bars indicate the maximum and minimum concentrations, and the upper and lower borders of the box mark the 75th and 25th percentile concentrations. The mean and median concentrations are shown as the open squares and solid lines within each column, respectively.

highest mean levels in the T3 zone. The ethyne level in T2 is relatively higher than that in T1, whereas the levels of propene and propane are comparable in both zones. For the remaining species, their levels are lower in T2 than in T1 (Fig. 2). The uneven distribution of both the local population activities and regional emissions from air pollutant sources that can be transported to Tibet could contribute to the observed differences.

3.2. Source category and distribution

In the PMF analysis, three source factors (Fig. 3a) are labeled according to the explained variability (EV) of their key tracer compounds, the relative contribution of each factor to the individual compounds, as their absolute mixing ratios in ambient air are on different scales and not directly comparable (Shim et al., 2007; Lanz et al., 2008). The first factor is dominated by large signals of BTEX (B: 47%, 7 pptv; T: 83%, 21 pptv; E: 84%, 7 pptv; and X: 83%, 12 pptv) with much higher concentrations of TEX followed by benzene. TEX are primarily derived from residential solvent usage and industry sources, especially the solvent-related industry (eg. shoemaking, furniture, adhesives, printing and painting) as shown by many studies (Yuan et al., 2010; He et al., 2015); and hence TEX are the common VOC species in urban regions (Tang et al., 2008; Gaur et al., 2016). Although benzene is usually associated with combustion processes, painting and industrial processes may represent additional sources (Choi et al., 2010). In our study, it is hard to resolve the urban and industrial emission sources due to the finite tracer set. Therefore, this factor is labeled as “industry/urban”. Because the emissions from various industries and urban sources are complex, high signals of ethyne (24%, 29 pptv), propene (20%, 8 pptv), propane (16%, 10 pptv), isopentane (31%, 23 pptv), and 2-methylpentane (44%, 10 pptv) are also observed in this factor. Mo et al. (2017) found high fraction of these species in the petrochemical industry profile resolved from the PMF model. The benzene to toluene (B/T) ratio, a good diagnostic indicator of different sources, is 0.32 in this factor, which is slightly higher than the ratios of solvent use emissions (0.01–0.3) and industrial emissions

(0.005–0.016) reported in the literatures (Barletta et al., 2005; Tan et al., 2012). This may due to the higher reaction speed of toluene with atmospheric radicals such as hydroxyl radicals (OH) than benzene during transportation from the emission area to our observed sites. There were no factories or workshops around our sampling sites, so the local anthropogenic emissions were unremarkable, and air pollutants should originate mainly from surrounding regions. CH₃Cl emissions are primarily generated by biomass burning (Shim et al., 2007). However, high fraction of CH₃Cl (12%, 35 pptv) was observed in the industry/urban factor, much higher than the global industrial source fraction of 4% (McCulloch et al., 1999). This is likely to be attributed to the background contribution because CH₃Cl itself has a high background level of about 0.53–0.55 ppbv (Montzka and Reimann, 2011). The similar results were also observed in the industrial/urban factor profile in the Transport and Chemical Evolution over the Pacific (TRACE-P) experiment. In that study, the researchers thought that the industrial plumes had been influenced by the biofuel combustion (Shim et al., 2007).

The second factor is characterized by the largest signals of CH₃Cl (74%, 223 pptv), which is a typical species from biomass burning sources (Blake et al., 2003; Shim et al., 2007). This factor also presents a large contribution to ethyne (44%, 53 pptv), propene (50%, 20 pptv), propane (60%, 36 pptv) and benzene (30%, 4 pptv). The factor profile matches well with the source profiles for biomass burning as reported by Liu et al. (2008). In those source profiles, ethyne, propene, propane and benzene are among the 10 most abundant VOCs species. B/T ratio in this factor is 1.92. Higher benzene emissions with respect to toluene have been reported for biofuel, charcoal and coal burning (Barletta et al., 2005). Considering all of above, this factor is assigned to the “biomass burning emission”. In urban areas, propene and propane mainly originate from the use of liquefied petroleum gas (LPG) and natural gas (NG) (Liu et al., 2016; Mo et al., 2017; He et al., 2015). However, smoldering biomass combustion may be a major source in rural areas (Ferek et al., 1998; Greenberg et al., 1984). The emission factors of propene and propane from the forest, cerrado and pasture fires

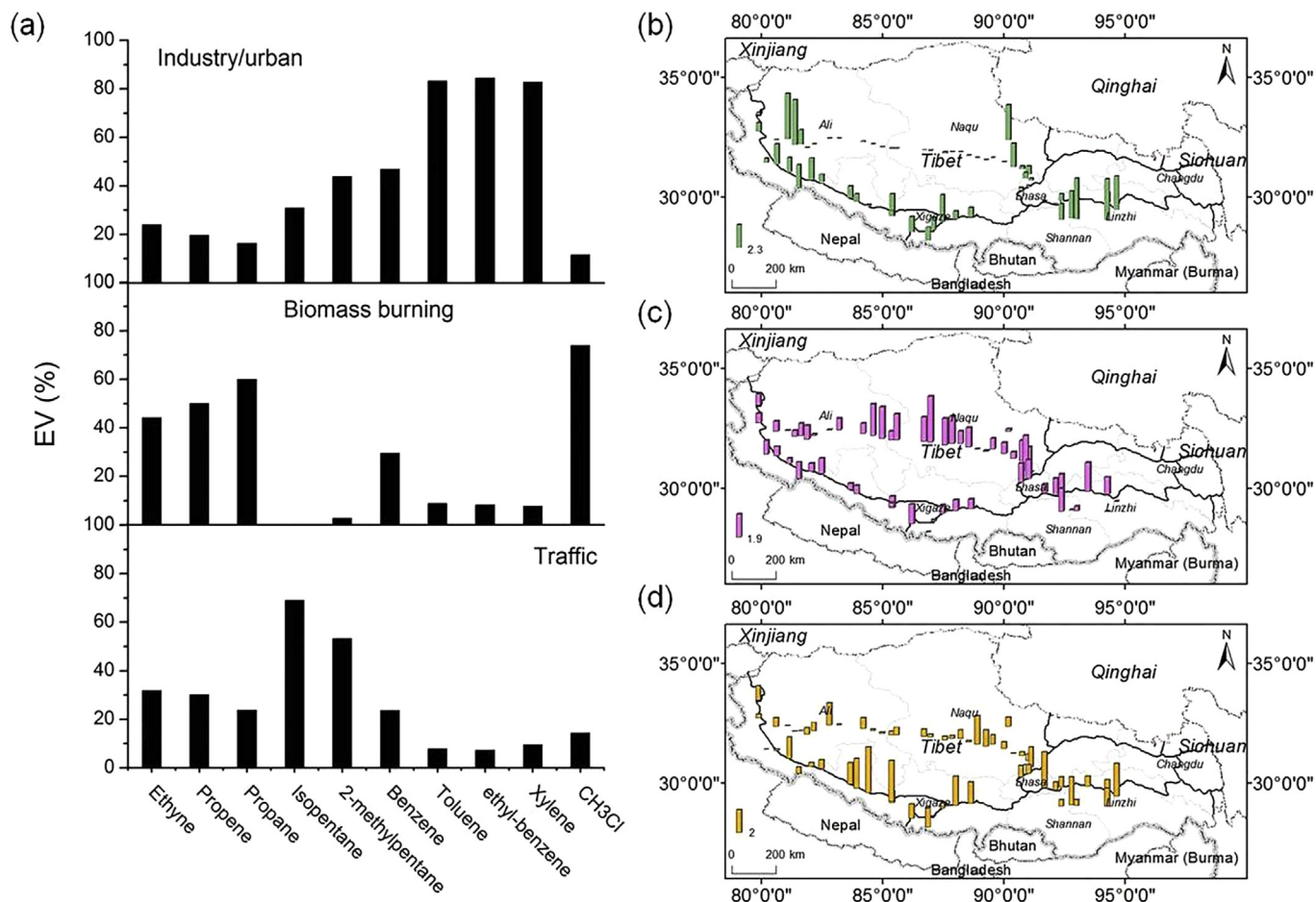


Fig. 3. Explained variations (%) of species in the PMF-identified source factors (a), and spatial distributions of factor contributions (avg = 1) (b–d). (b), Industry/urban source; (c), biomass burning source; and (d), traffic source.

were found to be about 1 and 0.3 g/kg C burned, and had good relationship with CO, a useful atmospheric tracer for incomplete combustion sources (Ferek et al., 1998).

Factor 3 has significant amounts of isopentane (69%, 51 pptv) and 2-methylpentane (53%, 12 pptv), both of which are markers for gasoline evaporation with high levels in the gasoline vapor profiles and vehicle exhaust profiles (He et al., 2015; Liu et al., 2008). This factor also has high loadings of ethyne (32%, 38 pptv), propene (30%, 12 pptv), propane (24%, 14 pptv), and benzene (24%, 3 pptv), which was also observed in the reported traffic source profiles (Liu et al., 2008). Therefore, factor 3 is identified as “traffic”. The traffic factor accounts for 14.36% of CH₃Cl (43.26 pptv). The reason may be similar with the industry/urban factor. Unexpectedly, the loading of toluene (24%, 1.98 pptv) in this factor is very low, and much lower than that of benzene with a high B/T ratio (1.73), which is also observed in the vehicle emission factor profiles resolved by other studies using PMF model (Liu et al., 2016; Mo et al., 2017). A B/T ratio of around 0.5 (wt/wt) has been reported to be characteristic of vehicular emissions (Barletta et al., 2005). Because toluene is more reactive than benzene, the B/T ratio will become larger as the VOCs get older in the atmosphere. The high ratio in this study may suggest that the species were not emitted in situ but aged/transported.

Fig. 3b–d shows the distribution pattern of the PMF-modeled source factors along with the sampling tracks (from Fig. 1b). For the industry source factor, the sites with high contributions are mainly distributed in the southeastern area and far-western areas

in the Ali prefecture, and they are also distributed in the middle southern area. The sites in the northern area present only limited contributions to this factor except for two samples from the Naqu prefecture close to Lhasa. For the biomass combustion source factor, the sites in the northern and eastern areas have high contributions, whereas the sites in the southern area have relatively low contributions. For the traffic source factor, the sites with high contributions are primarily located in the eastern and southern areas, whereas sites with low contributions are located in the westernmost and northwestern areas. The above results indicate that different zones in Tibet are influenced by different emission sources.

3.3. Implications of VOC origins

Fig. 4 shows the population and socioeconomic status of each county in Tibet. The population is sparse in Tibet, with most of the area having only 1–10 persons/km², although certain regions have an even lower population density. Although the urban population density of Lhasa is high (5837 persons/km²), the population density in the area surrounding Lhasa is low (Huang et al., 2013; Tibet Statistical Yearbook, 2009). Few industrial enterprises are located in Tibet, with fewer than ten located in the counties of Changdu, Linzhi, Shannan, Naqu and Ari, 12 located in Xigaze and 55 located in Lhasa. The Tibet Statistical Yearbook (2011) recorded only 6409 and 5161 km of traffic mileage in Changdu and Linzhi in 2010, respectively, and 23,000 and 110,000 vehicles in Linzhi and Lhasa,

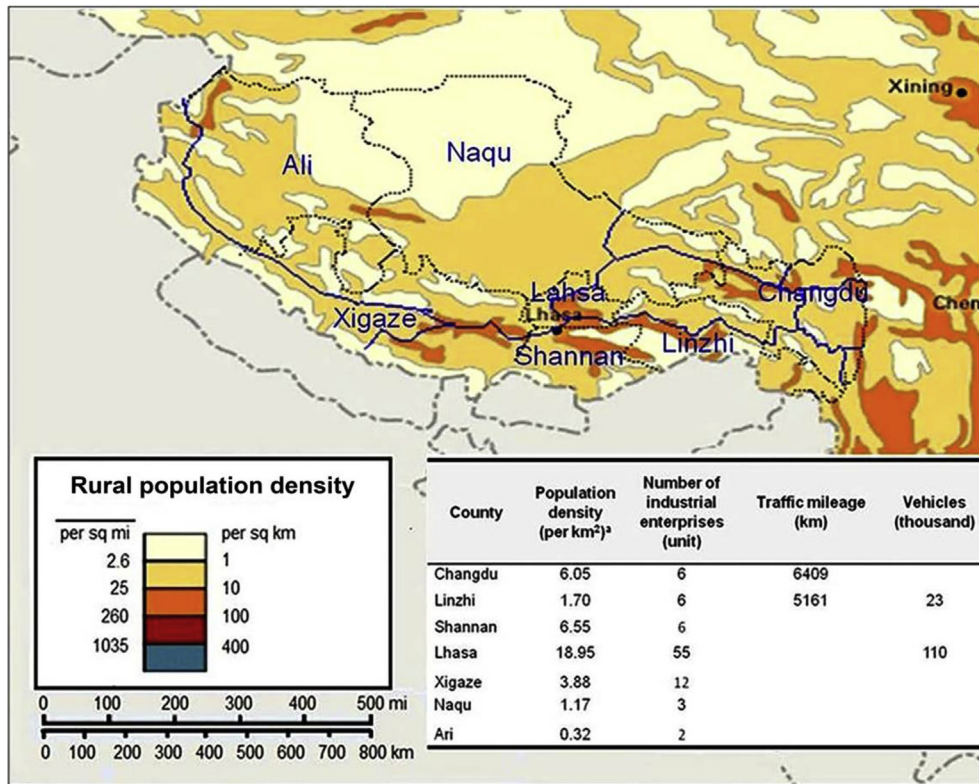


Fig. 4. Socioeconomic status of each county in Tibet. The population distribution map is modified based on the map shown in Britannica Online for Kids (<http://kids.britannica.com/comptons/art-143477>), whereas the data in the table are drawn from the *Tibet Statistical Yearbook* (2009).

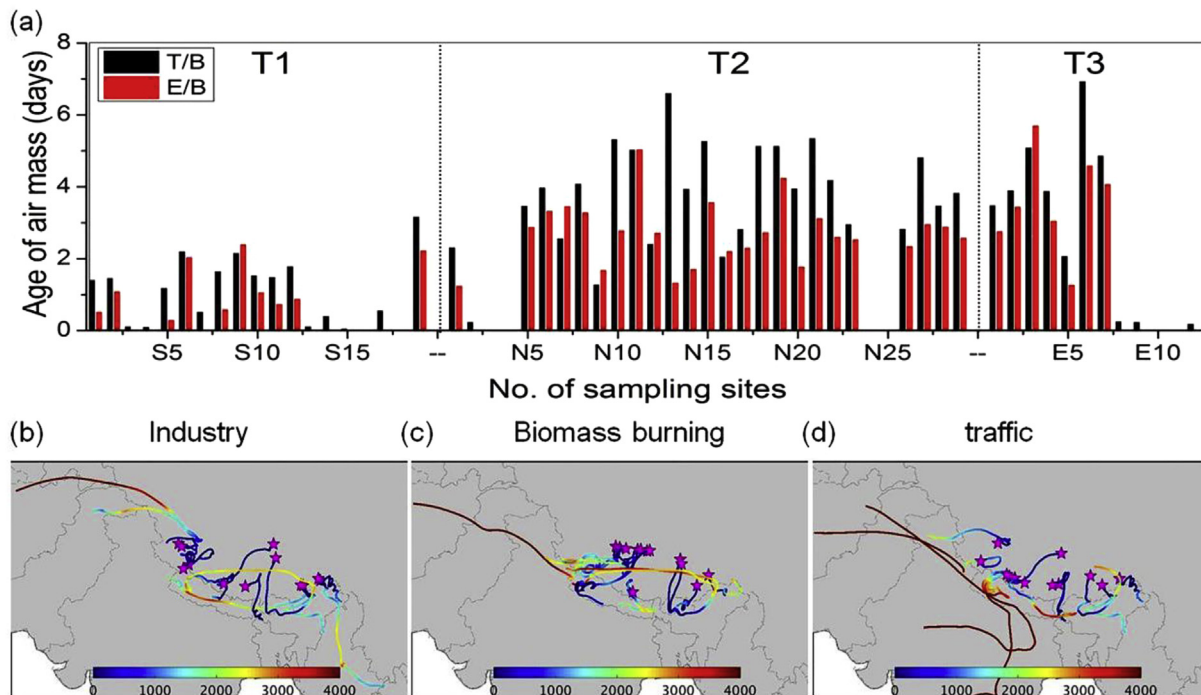


Fig. 5. Ages of the air masses at all sampling sites estimated using T/B and E/B ratios (a) and five-day back trajectories of the sites with the top 20% factor contributions for the industry (b), biomass burning (c) and traffic (d) sources in Tibet. The sampling sites of Track 1, which are distributed in southern Tibet, are numbered S1-S19, and those of Track 2 and Track 3, which are distributed in the northern and eastern areas of Tibet, respectively, are numbered N1-N29 and E1-E12, respectively, as shown in Table S1. The stars show the locations of the measurements. The colors of the air trajectories represent the height during transport. (For interpretation of the references to colour in this figure legend, the reader is referred to the web version of this article.)

respectively. Because of the low human activity in Tibet, the local emissions of VOCs should be limited, especially in the northern and western regions. A comparison of the distributions of the three different factors (Fig. 3b–d) with the population activities (Fig. 4) indicates that the factors are not consistent, especially the industry and biomass burning factors. This discrepancy indicates that local emissions may not have a major influence on VOC pollution in Tibet.

The air mass photochemical age at the sampling sites in Tibet is evaluated (Fig. 5) according to the method reported by Roukos et al. (2009) and Baker et al. (2011):

$$\tau = \left(\ln \left(\frac{[A]_0}{[D]_0} \right) - \ln \left(\frac{[A]_t}{[D]_t} \right) \right) / (k_A - k_D) \times [\text{OH}'] \quad (1)$$

where $[A]_0$ and $[D]_0$ are the initial concentrations of compound A and compound D at the emission sites (molecule/cm³), respectively; $[A]_t$ and $[D]_t$ are the final concentrations of the two compounds at the sampling sites (molecule/cm³), respectively; $[\text{OH}']$ is the ambient mixing ratio of OH' (molecule/cm³); k_A and k_D (cm³/molecules) are the reaction rate constants of A and D with OH', respectively; and τ is the time from emission to sampling (s).

The theory of this method is based on changes in the ratio between two compounds that have similar sources but different rates of reaction with OH'. This method removes the reliance on knowing the absolute mixing ratios of the VOCs at the source, and also accounts to some extent for dilution, which is expected to act equally on both VOCs, thereby having a smaller effect on the ratio than the absolute concentrations. However, some conditions need to be met when use it: (1) the two compounds should mainly come from the same source and be simultaneously introduced into the same air parcel; (2) background mixing ratios for the two VOC species should be negligible relative to their concentrations in the air parcel; (3) the compounds are primarily removed from the atmosphere by reactions with the OH' whereas the reactions with NO₃ and O₃ are neglected (Roukos et al., 2009; Baker et al., 2011). It was suggested that the applicability of this method could be estimated by comparing the estimates derived from two different VOC ratios, calculated from the measurements of three different VOCs, A, D and C. If a data set of VOCs compounds is collected in the same air parcel, and only reaction with OH' is acting on the ratios, the two estimates will be related by the following linear expression where the slope is only determined by the OH' rate constants (Parrish et al., 1992; Roukos et al., 2009):

$$\ln \left(\frac{[A]_t}{[D]_t} \right) = \frac{(k_A - k_D)}{(k_C - k_D)} \ln \left(\frac{[C]_t}{[D]_t} \right) + \left[\ln \left(\frac{[A]_0}{[D]_0} \right) - \frac{(k_A - k_D)}{(k_C - k_D)} \ln \left(\frac{[C]_0}{[D]_0} \right) \right] \quad (2)$$

In our study, the logarithms of [toluene]/[benzene] ([T]/[B]) and [ethylbenzene]/[benzene] ([E]/[B]) for most of the sampling sites show a good linear relationship (slope = 1.25, R² = 0.91; Fig. S1). The slope is quite close to the theoretical kinetic slope (1.3106, considering values of 1.22, 5.63 and 7.0 × 10¹² cm³ molecule⁻¹ s⁻¹ for k_B , k_T and k_E at 298 K, respectively) that we consider the photochemical estimates using the three aromatics to be valid.

Because India is the primary upwind area for Tibet, initial emission ratios of 2 for [T]₀/[B]₀ and 0.5 for [E]₀/[B]₀ are chosen, which are close to the values found in the atmosphere of Delhi, India, and represent the influence of urban emissions (Hoque et al., 2008; Singh et al., 2016). An [OH'] concentration of 10⁶ molecule/cm³ is used for the calculation. Finally, the estimated age of the air mass determined from [T]/[B] ranges from 0 to 6.9 days (Fig. 5a). Most of the sites in the south (T1) have an air mass age below two

days and an average age of 1.05 days, indicating that the air mass is relatively fresh and this area is mainly influenced by local emissions. Certain sites in the south of the T3 zone have similar ages. However, most of the sites in the northern (T2) and eastern (T3) areas have an air mass age greater than two days and an average age of 3.5 and 2.8 days, respectively. The results suggest that the VOC species in these areas are not emitted in situ but are chemically aged and likely transported to the region. Photochemical ages determined from [E]/[B] are slightly lower than the [T]/[B] ages, while the estimates from the two ratios are in fairly good agreement.

Because of the influence of strong westerlies during most of the year, Tibet is considered to be a receptor region for South Asian pollutants (Lu et al., 2012; Zhang et al., 2015). Although the Himalayas area “natural barrier” that can impede pollutants from reaching Tibet because of the high altitude, valleys in the Himalayan Mountains can serve as “leaking channels” that transport pollutants to Tibet through valleys such as the Yarlung Tsangpo River valley and Zhangmu valley (Wang et al., 2006, 2015). Pollutants can also be transported to Tibet directly via aerosol run-up from the IGP, which can reach up to 5–6 km in altitude (Wang et al., 2015; Xu et al., 2014; Xia et al., 2011). This altitude exceeds the height of most of the mountain valleys in the Himalayas. Several previous studies have found long-range atmospheric transport (LRAT) signs of BC, POPs, and PAHs in Tibet from South Asia and the Middle East because of the influence of the westerlies (Cong et al., 2015; Wang et al., 2006, 2015). Similarly, long-lived VOCs emitted in the upwind regions can be transported to Tibet.

It is important to note that there are large uncertainties associated with the estimates of photochemical processing, primarily dependent on the use of a highly averaged OH' level for such a highly variable species, and initial emission ratios from very few urban studies in India. As reported by Baker et al. (2011), uncertainties in [OH'] of ±25% correspond to transport times that are underestimated by 33% in the case of [OH'] being lower than the estimate, and a 20% overestimate in transport times if [OH'] is higher. Due to VOCs data for the upwind regions of Tibet are limited, which accordingly limit the certainty in the emissions ratios used in the transport time estimates. Smaller actual emission ratios would mean that predicted τ values are too high, while larger emission ratios would give τ values that are too low. For the photochemical ages greater than 0.5 d in this study, uncertainties in T/B and E/B ratios of ±50% correspond to transport times that are underestimated by 46.22 ± 39.37% and 43.77 ± 32.04% respectively, in the case of the two actual ratios being higher than their representative values we used, while a 63.13 ± 26.00% and 61.54 ± 24.58% overestimate in transport times if the two actual ratios are lower.

3.4. Potential source regions and transport pathways

The distributions of the three source factors in Tibet, i.e., industry/urban, biomass burning, and traffic, are inconsistent (section 3.2). To explore their respective source regions, the top 20% sampling sites for factor contributions are selected and used to calculate the five-day back trajectories using the HYSPLIT model (Fig. 5b–d). The related countries in the map are labeled in Fig. S2.

Three major source regions are identified for the LRAT of the industrial/urban factor as shown in Fig. 5b. *Region 1* corresponds to the transport from the northwest direction to the westernmost zone of Tibet, and the air masses pass through Afghanistan, Pakistan, and Tajikistan. Afghanistan is known for its petroleum industries. The region around the tracks in Pakistan likely includes several major cities, such as Islamabad, Rawalpindi, and Lahore, which suffer from serious air pollution related to industry and other

urban sources (Colbeck et al., 2010). Region 2 corresponds to the transport from the IGP to the southern-middle and northern-middle zones of Tibet. The IGP is a large river basin that presents the highest population and most serious pollution in the world. The basin cuts across several countries, including Pakistan, India, Nepal, and Bangladesh, and has a length of 1600 km and a width of 400 km (Dey and Di Girolamo, 2010). Population growth in this fluvial land form drives the rapid urbanization and development of various industries, including the iron and steel, electricity, cement, and chemical industries (Naja et al., 2014). Importantly, the air masses in the IGP always move along the southern edge of the Himalayas before they reach Tibet; thus, various pollutants are added to the air masses as they travel from the IGP into Tibet. Region 3 corresponds to the transport from Meghalaya (a northeastern state in India) and Myanmar to eastern Tibet. Although industrial development in Meghalaya and Myanmar is relatively slow, these areas produce higher VOC emissions than Tibet (Kurokawa et al., 2013); they are also surrounded and influenced by many polluted areas, such as India and other Southeast Asian countries.

The biomass burning factor is primarily related to transport from the IGP region to the middle-northern and eastern zones of Tibet (Fig. 5c). One array of air masses originates from northwest India, which represents a major agricultural base and produces approximately two-thirds of the country's food (Nasa, 2012). The other array of air masses originates from northeast India, where agriculture is also the primary industry. Each year, agricultural waste is commonly burned for crop rotation in October and March in the IGP region, thereby emitting large amounts of air pollutants, including VOCs (Fig. 6) (Dey and Di Girolamo, 2010; Xu et al., 2014). Our sampling period coincided with the Kharif crop harvest season (October) in India. Previous studies reported that smog aerosols emitted during large strong forest fires in northern India and the Himalayas can reach the planetary boundary layer and enter the central TP by deep convection and atmospheric circulation (Xu et al., 2014; Xia et al., 2011). In our study, the biomass burning influence the northern part more significantly, rather than the adjacent southern region. This is due to the peculiar meteorological conditions during the sampling period of northern samples. Our previous analysis of WRF-simulated surface wind speed found that there was a southeastward-moving upper-tropospheric cut-off low system which induced increasingly stronger surface wind from India to Tibet during 21–24 October, 2010 (Zhang et al., 2017). Trans-Himalaya air mass flux increased by a factor of 2–5 in the lower atmosphere, causing a more rapid and efficient pollutant transport pathway than transport pathways previously proposed

by other studies, such as westerlies (Cong et al., 2015; Ji et al., 2015) and mountain-valley winds (Hindman and Upadhyay, 2002; Dumka et al., 2010).

As shown in Fig. 5d, the data points with a high factor score for traffic are primarily centered on the national road 108 in southern Tibet. The age of air masses at those sites was as short as about 1 day as estimated in section 3.3. Therefore, the possibility of local emissions by the vehicles running on that road cannot be excluded. Meantime, the back trajectories reveal other possible source regions of the traffic-related pollutants in southern Tibet including the areas of northwest India, Nepal, Bangladesh, and Meghalaya of India close to Tibet. These areas include cities and abundant tourism resources, and also several important trading ports, such as Zhangmu and Jilong on the boundary between Nepal and Tibet, where present significant diesel vehicle traffic. Although several air mass trajectories pass through other areas with high traffic emissions, such as Afghanistan, Pakistan, and central India, their influence on Tibet should be small because the altitudes of the air masses are high (over 4000 m).

4. Conclusions

VOCs distributed across Tibet are sampled and analyzed in this study, and the results show that although Tibet is still a relatively clean region, the Tibetan atmosphere has been influenced by anthropogenic activities. The highest VOC level is observed in the eastern region (T3), followed by the southern region (T1) and the northern region (T2). A suite of trace chemicals, including ethyne, propene, propane, i-pentane, 2-methylpentane, BTEX, and CH_3Cl , are chosen as proxies to diagnose source regions and related transport of pollutants to Tibet. Three factors (traffic, biomass burning, and industry/urban) are identified by PMF analysis that have different distribution characteristics in Tibet. The sampling sites located in southern Tibet receive a large contribution of VOCs from the traffic and industry/urban factors, whereas the northern sites receive a large contribution of VOCs from the biomass burning factor. Foreign emission sources have a higher probability of influencing the Tibetan air than local sources in the northern and eastern regions, which present an air mass that is older than two days. Back-trajectory analyses indicate that industry-related VOC pollutants in Tibet have three source regions: the Afghanistan-Pakistan-Tajikistan region, the IGP, and the Meghalaya-Myanmar region. Biomass burning-related pollutants are associated with the transport from agricultural bases in northern India. The traffic-related pollutants mainly originate from local and neighboring

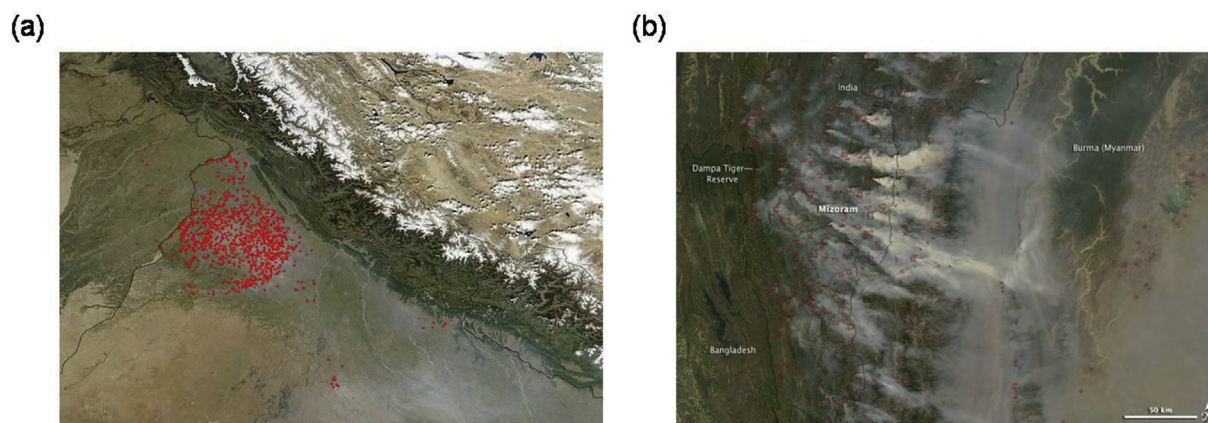


Fig. 6. Agricultural fires in northwest India (a) and northeast India (b). The two images were captured by NASA during the crop seasons in India. Sources: (a) http://www.nasa.gov/mision_pages/fires/main/world/20111031-india.html; and (b) <http://earthobservatory.nasa.gov/NaturalHazards/view.php?id=85500>.

areas, including northwest India, Nepal, Bangladesh and Meghalaya (India). The most striking result of our study is the precise identification of source regions that appear to significantly contribute to VOC emissions and air pollution over different zones of Tibet, which can help us to better understand the origin of BC in Tibet. Previous studies demonstrated that the origin of air pollutants in Tibet presented seasonal variations due to the influence of the Indian monsoon system (Kopacz et al., 2011; Zhang et al., 2015). Our study, which was conducted in October, captures the non-monsoon season. An important extension of this work will be to perform similar analyses to make up the seasonal sampling gap.

Acknowledgments and data

The work was funded by the National Natural Science Foundation of China (No. 41501543, 41472311, 41273107), the Shanxi Province Science Foundation for Youths (No. 2015021059) and the Special Scientific Research Funds for Environmental Protection Commonwealth Section (20603020802L). The authors duly acknowledge the partial support received from the One-hundred Talent Program, which is supported by the Organization Department of Shanxi Province Committee. The authors also thank the NOAA Air Resources Laboratory (ARL) for providing the HYSPLIT model.

Appendix A. Supplementary data

Supplementary data related to this article can be found at <http://dx.doi.org/10.1016/j.atmosenv.2017.07.031>.

References

- Baker, A.K., Schuck, T.J., Slemr, F., van Velthoven, P., Zahn, A., Brenninkmeijer, C.A.M., 2011. Characterization of non-methane hydrocarbons in Asian summer monsoon outflow observed by the CARIBIC aircraft. *Atmos. Chem. Phys.* 11, 503–518. <http://dx.doi.org/10.5194/acp-11-503-2011>.
- Barletta, B., Meinardi, S., Rowland, F.S., Chan, C.Y., Wang, X., Zou, S., Chan, L.Y., Blake, D.R., 2005. Volatile organic compounds in 43 Chinese cities. *Atmos. Environ.* 39, 5979–5990. <http://dx.doi.org/10.1016/j.atmosenv.2008.01.028>.
- Blake, N.J., Blake, D.R., Simpson, I.J., Meinardi, S., Swanson, A.L., Lopez, J.P., Katzenstein, A.S., Barletta, B., Shirai, T., Atlas, E., Sachse, G., Avery, M., Vay, S., Fuelberg, H.E., Kiley, C.M., Kita, K., Rowland, F.S., 2003. NMHCs and halocarbons in Asian continental outflow during the transport and chemical evolution over the Pacific (TRACE-P) field campaign: comparison with PEM-west B. *J. Geophys. Res.* 108, 8806. <http://dx.doi.org/10.1029/2002JD003367>.
- Bond, T.C., Bhardwaj, E., Dong, R., Jogani, R., Jung, S., Roden, C., Streets, D.G., Trautmann, N.M., 2007. Historical emissions of black and organic carbon aerosol from energy-related combustion, 1850–2000. *Glob. Biogeochem. Cy.* 21, GB2018. <http://dx.doi.org/10.1029/2006GB002840>.
- Cao, J., Tie, X., Xu, B., Zhao, Z., Zhu, C., Li, G., Liu, S., 2010. Measuring and modeling black carbon (BC) contamination in the SE Tibetan Plateau. *J. Atmos. Chem.* 67, 45–60. <http://dx.doi.org/10.1007/s10874-011-9202-5>.
- Choi, E., Heo, J.B., Yi, S.M., 2010. Apportioning and locating nonmethane hydrocarbon sources to a background site in Korea. *Environ. Sci. Technol.* 44, 5849–5854. <http://dx.doi.org/10.1021/es903634e>.
- Colbeck, I., Nasir, Z.A., Ali, Z., 2010. The state of ambient air quality in Pakistan—a review. *Environ. Sci. Pollut. Res.* 17, 49–63. <http://dx.doi.org/10.1007/s11356-009-0217-2>.
- Cong, Z., Kawamura, K., Kang, S., Fu, P., 2015. Penetration of biomass-burning emissions from South Asia through the Himalayas: new insights from atmospheric organic acids. *Sci. Rep.* 5. <http://dx.doi.org/10.1038/srep09580>.
- Dey, S., Di Girolamo, L., 2010. A climatology of aerosol optical and microphysical properties over the Indian subcontinent from 9 years (2000–2008) of Multi-angle Imaging Spectroradiometer (MISR) data. *J. Geophys. Res.* 115, D15204. <http://dx.doi.org/10.1029/2009JD013395>.
- Dumka, U.C., Moorthy, K.K., Kumar, R., Hegde, P., Sagar, R., Pant, P., Singh, N., Babu, S.S., 2010. Characteristics of aerosol black carbon mass concentration over a high altitude location in the Central Himalayas from multi-year measurements. *Atmos. Res.* 96, 510–521. <http://dx.doi.org/10.1016/j.atmosres.2009.12.010>.
- Ferek, R.J., Reid, J.S., Hobbs, P.V., Blake, D.R., Lioussis, C., 1998. Emission factors of hydrocarbons, halocarbons, trace gases and particles from biomass burning in Brazil. *J. Geophys. Res.* 103, 32107–32118. <http://dx.doi.org/10.1029/98JD00692>.
- Gaur, M., Singh, R., Shukla, A., 2016. Volatile Organic Compounds in India: concentration and Sources. *Gaur et al. J. Civ. Environ. Eng.* 6, 5. <http://dx.doi.org/10.4172/2165-784X.1000251>.
- Greenberg, J.P., Zimmerman, P.R., Heidt, L., Pollock, W., 1984. Hydrocarbon and carbon monoxide emissions from biomass burning in Brazil. *J. Geophys. Res.* 89, 1350–1354. <http://dx.doi.org/10.1029/JD089iD01p01350>.
- He, Q., Yan, Y., Li, H., Zhang, Y., Chen, L., Wang, Y., 2015. Characteristics and reactivity of volatile organic compounds from non-coal emission sources in China. *Atmos. Environ.* 115, 153–162. <http://dx.doi.org/10.1016/j.atmosenv.2015.05.066>.
- Hellén, H., Leck, C., Paatero, J., Virkkula, A., Hakola, H., 2012. Summer concentrations of NMHCs in ambient air of the arctic and antarctic, boreal. *Environ. Res.* 17, 385–397. Available at: <http://www.borenav.net/BER/pdfs/preprints/Hellen.pdf>.
- Helmig, D., Tanner, D.M., Honrath, R.E., Owen, R.C., Parrish, D.D., 2008. Nonmethane hydrocarbons at pico mountain, azores: oxidation chemistry in the north atlantic region. *J. Geophys. Res.* 113, D20S91. <http://dx.doi.org/10.1029/2007JD008930>.
- Hindman, E.E., Upadhyay, B.P., 2002. Air pollution transport in the Himalayas of Nepal and Tibet during the 1995–1996 dry season. *Atmos. Environ.* 36, 727–739. [http://dx.doi.org/10.1016/S1352-2310\(01\)00495-2](http://dx.doi.org/10.1016/S1352-2310(01)00495-2).
- Hoque, R.R., Khillare, P.S., Agarwal, T., 2008. Spatial and temporal variation of BTEX in the urban atmosphere of Delhi, India. *Sci. Total Environ.* 392, 30–40. <http://dx.doi.org/10.1016/j.scitotenv.2007.08.036>.
- Huang, J., Kang, S., Wang, S., Wang, L., Zhang, Q., Guo, J., Wang, K., Zhang, G., Tripathi, L., 2013. Wet deposition of mercury at Lhasa, the capital city of Tibet. *Sci. Total Environ.* 447, 123–132. <http://dx.doi.org/10.1016/j.scitotenv.2013.01.003>.
- Ji, Z., Kang, S., Cong, Z., Zhang, Q., Yao, T., 2015. Simulation of carbonaceous aerosols over the Third Pole and adjacent regions: distribution, transportation, deposition, and climatic effects. *Clim. Dynam.* 45, 2831–2846. <http://dx.doi.org/10.1007/s00382-015-2509-1>.
- Kang, S., Huang, J., Wang, F., Zhang, Q., Zhang, Y., Li, C., Wang, L., Chen, P., Sharma, C.M., Li, Q., Sillanpää, M., Hou, J., Xu, B., Guo, J., 2016. Atmospheric mercury depositional chronology reconstructed from lake sediments and ice core in the Himalayas and Tibetan plateau. *Environ. Sci. Technol.* 50, 2859–2869. <http://dx.doi.org/10.1021/acs.est.5b04172>.
- Kaspari, S.D., Schwikowski, M., Gysel, M., Flanner, M.G., Kang, S., Hou, S., Mayewski, P.A., 2011. Recent increase in black carbon concentrations from a Mt. Everest ice core spanning 1860–2000 AD. *Geophys. Res. Lett.* 38, L04703. <http://dx.doi.org/10.1029/2010GL046096>.
- Kopacz, M., Mauzerall, D.L., Wang, J., Leibensperger, E.M., Henze, D.K., Singh, K., 2011. Origin and radiative forcing of black carbon transported to the Himalayas and Tibetan Plateau. *Atmos. Chem. Phys.* 11, 2837–2852. <http://dx.doi.org/10.5194/acp-11-2837-2011>.
- Kurokawa, J., Ohara, T., Morikawa, T., Hanayama, S., Janssens-Maenhout, G., Fukui, T., Kawashima, K., Akimoto, H., 2013. Emissions of air pollutants and greenhouse gases over Asian regions during 2000–2008: regional Emission inventory in Asia (REAS) version 2. *Atmos. Chem. Phys.* 13, 11019–11058. <http://dx.doi.org/10.5194/acp-13-11019-2013>.
- Lanz, V.A., Hueglin, C., Vollmer, M.K., Steinbacher, M., Henne, S., Staehelin, J., Henne, S., Staehelin, J., Buchmann, B., Reimann, S., 2008. Statistical analysis of non-methane hydrocarbon variability at a European background location (Jungfraujoch, Switzerland). *Atmos. Chem. Phys. Discuss.* 8, 19527–19559. <http://dx.doi.org/10.5194/acpd-8-19527-2008>.
- Li, C., Bosch, C., Kang, S., Andersson, A., Chen, P., Zhang, Q., Cong, Z., Chen, B., Qin, D., Gustafsson, Ö., 2016. Sources of black carbon to the Himalayan–Tibetan plateau glaciers. *Nat. Commun.* 7, 12574. <http://dx.doi.org/10.1038/ncomms12574>.
- Li, J., Zhu, T., Wang, F., Qiu, X.H., Lin, W.L., 2006. Observation of organochlorine pesticides in the air of the Mt. Everest region. *Ecotoxicol. Environ. Saf.* 63, 33–41. <http://dx.doi.org/10.1016/j.ecoenv.2005.04.001>.
- Liu, B., Liang, D., Yang, J., Dai, Q., Bi, X., Feng, Y., Yuan, J., Xiao, Z., Zhang, Y., Xu, H., 2016. Characterization and source apportionment of volatile organic compounds based on 1-year of observational data in Tianjin, China. *Environ. Pollut.* 218, 757–769. <http://dx.doi.org/10.1016/j.envpol.2016.07.072>.
- Liu, Y., Shao, M., Fu, L., Lu, S., Zeng, L., Tang, D., 2008. Source profiles of volatile organic compounds (VOCs) measured in China: Part I. *Atmos. Environ.* 42, 6247–6260. <http://dx.doi.org/10.1016/j.atmosenv.2008.01.070>.
- Lu, Z., Streets, D.G., Zhang, Q., Wang, S., 2012. A novel back-trajectory analysis of the origin of black carbon transported to the Himalayas and Tibetan Plateau during 1996–2010. *Geophys. Res. Lett.* 39, L01809. <http://dx.doi.org/10.1029/2011GL049903>.
- McCulloch, A., Michael, L.A., Carmen, M.B., Thomas, E.G., Gary, K., Pauline, M.M., Li, Y.F., 1999. Global emissions of hydrogen chloride and chloromethane from coal combustion, incineration, and industrial activities: reactive chlorine emissions inventory. *J. Geophys. Res.* 104, 8391–8403. <http://dx.doi.org/10.1029/1999JD900025>.
- Ming, J., Xiao, C., Sun, J., Kang, S., Bonasoni, P., 2010. Carbonaceous particles in the atmosphere and precipitation of the Nam Co region, central Tibet. *J. Environ. Sci.* 22, 1748–1756. [http://dx.doi.org/10.1016/S1001-0742\(09\)60315-6](http://dx.doi.org/10.1016/S1001-0742(09)60315-6).
- Ming, J., Cachier, H., Xiao, C., Qin, D., Kang, S., Hou, S., Xu, J., 2008. Black carbon record based on a shallow Himalayan ice core and its climatic implications. *Atmos. Chem. Phys.* 8, 1343–1352. <http://dx.doi.org/10.5194/acp-8-1343-2008>.
- Mo, Z., Shao, M., Lu, S., Niu, H., Zhou, M., Sun, J., 2017. Characterization of non-methane hydrocarbons and their sources in an industrialized coastal city, Yangtze River Delta, China. *Sci. Total Environ.* 593–594, 641–653. <http://dx.doi.org/10.1016/j.scitotenv.2017.03.123>.
- Montzka, S.A., Reimann, S., 2011. Ozone-depleting Substances (ODSs) and Related Chemicals. *Scientific Assessment of Ozone Depletion: 2010, Chapter 1. World*

- Meteorological Organization, Geneva, Switzerland, pp. 1–108.
- Naja, M., Mallik, C., Sarangi, T., Sheel, V., Lal, S., 2014. SO₂ measurements at a high altitude site in the central Himalayas: role of regional transport. *Atmos. Environ.* 99, 392–402. <http://dx.doi.org/10.1016/j.atmosenv.2014.08.031>.
- Nasa, 2012. Fires in Northern India. http://www.Nasa.gov/mission_pages/fires/main/world/20121031-india.html.
- Ohara, T., Akimoto, H., Kurokawa, J., Horii, N., Yamaj, K., Yan, X., Hayasaka, T., 2007. An Asian emission inventory of anthropogenic emission sources for the period 1980–2020. *Atmos. Chem. Phys.* 7, 4419–4444. <http://dx.doi.org/10.5194/acp-7-4419-2007>.
- Parrish, D.D., Hahn, C.J., Williams, E.J., Norton, R.B., Fehsenfeld, F.C., Singh, H.B., Shetter, J.D., Gandrud, B.W., Ridley, B.A., 1992. Indications of photochemical histories of Pacific air masses from measurements of atmospheric trace species at Point Arena, California. *J. Geophys. Res.* 97, 15883–15901. <http://dx.doi.org/10.1029/92JD01242>.
- Qiu, J., 2008. The third pole. *Nature* 454, 393–396. <http://dx.doi.org/10.1038/454393a>.
- Roukos, J., Riffault, V., Locoge, N., 2009. VOC in an urban and industrial harbor on the French North Sea coast during two contrasted meteorological situations. *Environ. Pollut.* 157, 3001–3009. <http://dx.doi.org/10.1016/j.envpol.2009.05.059>.
- Rubin, J.L., Kean, A.J., Harley, R.A., Millet, D.B., Goldstein, A.H., 2006. Temperature dependence of volatile organic compound evaporative emissions from motor vehicles. *J. Geophys. Res.* 111, D03305. <http://dx.doi.org/10.1029/2005JD006458>.
- Sarkar, C., Chatterjee, A., Majumdar, D., Ghosh, S.K., Srivastava, A., Raha, S., 2014. Volatile organic compounds over Eastern Himalaya, India: temporal variation and source characterization using Positive Matrix Factorization. *Atmos. Chem. Phys. Discuss.* 14, 32133–32175. <http://dx.doi.org/10.5194/acpd-14-32133-2014>.
- Sarkar, C., Sinha, V., Sinha, B., Panday, A.K., Rupakheti, M., Lawrence, M.G., 2017. Source apportionment of NMVOCs in the Kathmandu Valley during the SusKat-ABC international field campaign using positive matrix factorization. *Atmos. Chem. Phys. Discuss.* <http://dx.doi.org/10.5194/acp-2016-1139>.
- Shim, C., Wang, Y., Singh, H.B., Blake, D.R., Guenther, A.B., 2007. Source characteristics of oxygenated volatile organic compounds and hydrogen cyanide. *J. Geophys. Res.* 112, D10305. <http://dx.doi.org/10.1029/2006JD007543>.
- Singh, D., Kumar, A., Singh, B.P., Anandam, K., Singh, M., Mina, U., Kumar, K., Jain, V.K., 2016. Spatial and temporal variability of VOCs and its source estimation during rush/non-rush hours in ambient air of Delhi, India. *Air Qual. Atmos. Health.* 9, 483–493. <http://dx.doi.org/10.1007/s11869-015-0354-3>.
- Tan, J.H., Guo, S.J., Ma, Y.L., Yang, F.M., He, K.B., Yu, Y.C., Wang, J.W., Shi, Z.B., Chen, G.C., 2012. Non-methane hydrocarbons and their ozone formation potentials in Foshan, China. *Aerosol Air Qual. Res.* 12, 387–398. <http://dx.doi.org/10.4209/aaqr.2011.08.0127>.
- Tang, J.H., Chan, L.Y., Chang, C.C., Liu, S., Li, Y.S., 2009. Characteristics and sources of non-methane hydrocarbons in background atmospheres of eastern, south-western, and southern China. *J. Geophys. Res.* 114, D03304. <http://dx.doi.org/10.1029/2008JD010333>.
- Tang, J.H., Chan, L.Y., Chan, C.Y., Li, Y.S., Chang, C.C., Wang, X.M., Zou, S.C., Barletta, B., Blake, D.R., Wu, D., 2008. Implications of changing urban and rural emissions on nonmethane hydrocarbons in the Pearl River Delta region of China. *Atmos. Environ.* 42, 3780–3794. <http://dx.doi.org/10.1016/j.atmosenv.2007.12.069>.
- Tibet Statistical Yearbook, 2009. *Tabulation on the 2008 Population Census of Tibet by County, China*. statistical Publishing, 2009. 06, ISBN 978-7-5037-5678-8/C.2205.
- Tibet Statistical Yearbook, 2011. *Tabulation on the 2008 Population Census of Tibet by County, China*. statistical Publishing, 2011. 06, ISBN 978-7-5037-5678-8/C.2205.
- US EPA (U.S. Environmental Protection Agency), 2014. EPA Positive Matrix Factorization (PMF) 5.0 Fundamentals and User Guide. <http://www.epa.gov/head/research/pmf.html> (accessed in May 2015).
- Wang, M., Xu, B., Wang, N., Cao, J., Tie, X., Wang, H., Zhu, C., Yang, W., 2016. Two distinct patterns of seasonal variation of airborne black carbon over Tibetan Plateau. *Sci. Total Environ.* 573, 1041–1052. <http://dx.doi.org/10.1016/j.scitotenv.2016.08.184>, 2016.
- Wang, T., Guo, H., Blake, D.R., Kwok, Y.H., Simpson, I.J., Li, Y.S., 2005. Measurements of trace gases in the inflow of South China Sea background air and outflow of regional pollution at Tai O, Southern China. *J. Atmos. Chem.* 52, 295–317. <http://dx.doi.org/10.007/s10874-005-2219-x>.
- Wang, X., Gong, P., Sheng, J., Joswiak, D.R., Yao, T., 2015. Long-range atmospheric transport of particulate Polycyclic Aromatic Hydrocarbons and the incursion of aerosols to the southeast Tibetan Plateau. *Atmos. Environ.* 115, 124–131. <http://dx.doi.org/10.1016/j.atmosenv.2015.04.050>.
- Wang, X., Yao, T., Cong, Z., Yan, X., Kang, S., Zhang, Y., 2006. Gradient distribution of persistent organic contaminants along northern slope of central-Himalayas, China. *Sci. Total Environ.* 372, 193–202. <http://dx.doi.org/10.1016/j.scitotenv.2006.09.008>.
- Wang, Y., Shim, C., Blake, N., Blake, D., Choi, Y., Ridley, B., Dibb, J., Wimmers, A., Moody, J., Flocke, F., Weinheimer, A., Talbot, R., Atlas, E., 2003. Intercontinental transport of pollution manifested in the variability and seasonal trend of springtime O₃ at northern mid and high latitudes. *J. Geophys. Res.* 108 (4683), D21. <http://dx.doi.org/10.1029/2003JD003592>.
- Xia, X., Zong, X., Cong, Z., Chen, H., Kang, S., Wang, P., 2011. Baseline continental aerosol over the central Tibetan plateau and a case study of aerosol transport from South Asia. *Atmos. Environ.* 45, 7370–7378. <http://dx.doi.org/10.1016/j.atmosenv.2014.11.060>.
- Xiao, Q., Saikawa, E., Yokelson, R.J., Chen, P., Li, C., Kang, S., 2015. Indoor air pollution from burning yak dung as a household fuel in Tibet. *Atmos. Environ.* 102, 406–412. <http://dx.doi.org/10.1016/j.atmosenv.2014.11.060>.
- Xu, C., Ma, Y.M., Pandey, A., Cong, Z.Y., Yang, K., Zhu, Z.K., Wang, J.M., Amatya, P.M., Zhao, L., 2014. Similarities and differences of aerosol optical properties between southern and northern sides of the Himalayas. *Atmos. Chem. Phys.* 14, 3133–3149. <http://dx.doi.org/10.5194/acp-14-3133-2014>.
- Yang, K., Wu, H., Qin, J., Lin, C., Tang, W., Chen, Y., 2014. Recent climate changes over the Tibetan Plateau and their impacts on energy and water cycle: a review. *Glob. Planet. Change* 112, 79–91. <http://dx.doi.org/10.1016/j.gloplacha.2013.12.001>.
- Yao, T., Thompson, L., Yang, W., Yu, W., Gao, Y., Guo, X., Yang, X., Duan, K., Zhao, H., Xu, B., Pu, J., Lu, A., Xiang, Y., Kattel, D.B., Joswiak, D., 2012. Different glacier status with atmospheric circulations in Tibetan Plateau and surroundings. *Nat. Clim. Change* 2, 663–667. <http://dx.doi.org/10.1038/nclimate1580>.
- Yuan, B., Shao, M., Lu, S.H., Wang, B., 2010. Source profiles of volatile organic compounds associated with solvent use in Beijing, China. *Atmos. Environ.* 44, 1919–1926. <http://dx.doi.org/10.1016/j.atmosenv.2010.02.014>.
- Zhang, R., Wang, H., Qian, Y., Rasch, P.J., Easter, R.C., Ma, P.L., Singh, B., Huang, J., Fu, Q., 2015. Quantifying sources, transport, deposition, and radiative forcing of black carbon over the Himalayas and Tibetan Plateau. *Atmos. Chem. Phys.* 15, 6205–6223. <http://dx.doi.org/10.5194/acp-15-6205-2015>.
- Zhang, R.X., Wang, Y.H., He, Q.S., Chen, L.G., Zhang, Y.Z., Qu, H., Smeltzer, C., Li, J.F., Leonardo, M.A.A., Mihalis, V., Andreas, R., Folkard, W., John, P.B., 2017. Enhanced trans-Himalaya pollution transport to the Tibetan Plateau by cut-off low systems. *Atmos. Chem. Phys.* 17, 3083–3095. <http://dx.doi.org/10.5194/acp-17-3083-2017>.
- Zhang, Y., Wang, X., Blake, D.R., Li, L., Zhang, Z., Wang, S., Guo, H., Lee, F.S.C., Gao, B., Chan, L., Wu, D., Rowland, F.S., 2012. Aromatic hydrocarbons as ozone precursors before and after outbreak of the 2008 financial crisis in the Pearl River Delta region, south China. *J. Geophys. Res.* 117, D15306. <http://dx.doi.org/10.1029/2011JD017356>.
- Zhao, Z., Cao, J., Shen, Z., Xu, B., Zhu, C., Chen, L.W.A., Su, X., Liu, S., Han, Y., Wang, G., Ho, K., 2013. Aerosol particles at a high-altitude site on the southeast tibetan plateau, China: implications for pollution transport from South Asia. *J. Geophys. Res.* 118, 11360–11375. <http://dx.doi.org/10.1002/jgrd.50599>.